

Self-decoupling elements of 8-channel 7T head antenna

H. Habara¹, Y. Bito¹, H. Ochi¹, Y. Soutome¹, Y. Kaneko¹, M. Dohata^{1,2}, H. Takeuchi², and T. Takahashi²

¹Central Research Lab., Hitachi Ltd., Kokubunji, Tokyo, Japan, ²Hitachi Medical Corporation, Kashiwa, Chiba, Japan

Introduction

Multichannel transmit antennas are gaining importance for higher field MRI, because RF shimming and transmit sense methods are very effective for correcting B_1 inhomogeneity. To fabricate a multichannel antenna, loop antennas [1], degenerated birdcages, and microstrip line antennas (or TEM) [2] have been used. Loop antennas have low self-resonance frequency so ingenuity is needed to use them in higher fields. Decoupling in multichannel microstrip line is difficult in high field antenna design. The decoupling capacitor value for the microstrip line tends to be too small, below 1 pF for a 7T-head-sized antenna. Therefore, an inductively decoupled microstrip line has been tested [3]. A microstrip line with meander conductors in both ends was recently reported to improve decoupling efficiency by 2 dB [4].

For more effective decoupling methods, we introduce meandering or snaking elements to replace linear conductive elements such as a microstrip line. To show the effectiveness of this replacement, the decoupling performance of the snaking elements was compared with that of the microstrip line.

Method

Eight channel 7T head volume antennas were designed to include snaking elements. A normal microstrip line element antenna was also modeled for comparison. The snaking elements had 12-mm wide conductors, 48-mm side-by-side snaking width, and a 44-mm Z-direction repetition pitch (Fig. 1(a)). A cylindrical RF shield had a 290-mm diameter and 240-mm length. The conductive elements with a 220-mm Z-direction length are placed at a 15-mm inner cylindrical surface from the RF shield. For the microstrip line model, the conductor was 20-mm wide, and 10-mm wide decoupling wings were attached to one end of each rung (Fig. 1(b)). The sensitivity and the S-parameters were calculated at 300 MHz using CST studio suite®. Feeding points were placed in the centers of the rungs with matching capacitors. A model of an average Japanese woman, Hanako [5], with a 4mm cube mesh, was loaded into the antennas.

Results and discussion

The decoupling capacitor value was only 0.15 pF for the microstrip line model, achieving the S_{12} parameter of -12 dB with the nearest neighborhood elements. The snaking elements decoupled by themselves to the nearest neighborhood by -12 dB without any decoupling capacitors. Figure 2 shows B_1^+ maps at one-channel feeding for the snaking elements (Fig. 2(a)) and the microstrip line (Fig. 2(b)). The microstrip line element weakly couples to the 1st, 2nd, and 4th neighborhood elements. In contrast, a snaking element couples weakly only to the 1st neighborhood elements. Figure 3 shows 8-channel equally phase (45°)-shifted drive B_1^+ maps for the two models. The mean distance between the diagonal pairs of the eight sensitivity dips was 238 mm in the snaking elements, which is longer than the value (222 mm) in the microstrip line. Therefore, a larger imaging region is available in the snaking element model than in the microstrip line model. Figure 4 illustrates the self decoupling characteristics of the snaking elements. The magnetic field line ejects from a triangle-shaped cutout and is absorbed in the next vicinity cutout in the snaking elements. Therefore, the spreading of the magnetic field line to the neighboring elements is less in the snaking elements than in the microstrip line. This illustrates the self decoupling nature of snaking elements.

References

- [1] V. Alagappan et al., Proc. Intl. Soc. Mag. Reson. Med. 17, p. 3008 (2009)
- [2] G. Adriany et al., Mag. Reson. Med. 53: 434-445 (2005)
- [3] B. Wu et al., J. Mag. Reson. 182: 126-132 (2006)
- [4] S. Orzada et al., Proc. Intl. Soc. Mag. Reson. Med. 17, p. 3010 (2009)
- [5] T. Nagaoka et al., Physics in Medicine and Biology, 49, 1-15 (2004)

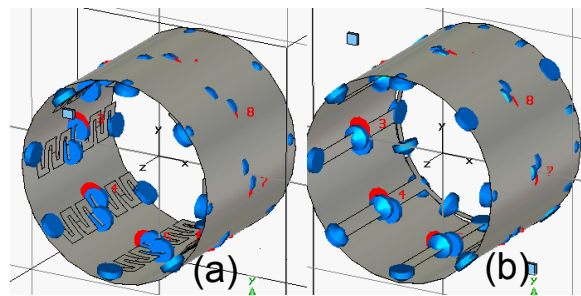


Fig. 1 Feed (red) and capacitors (blue) of snaking element antenna (a) and microstrip line antenna (b)

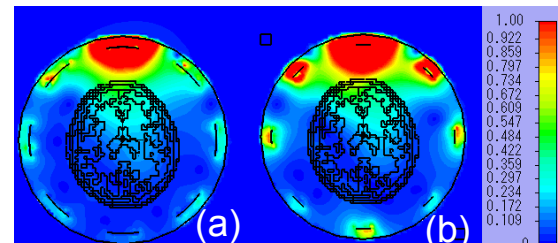


Fig. 2 One-channel drive B_1^+ map of snaking element antenna (a) and microstrip line antenna (b)

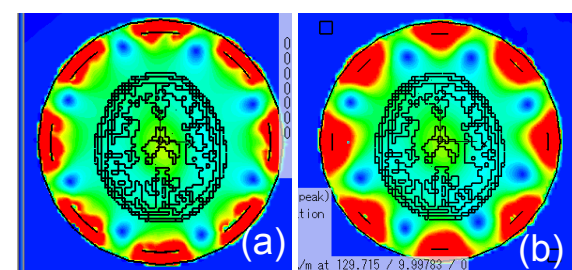


Fig. 3 Eight-channel drive B_1^+ map of snaking element antenna (a) and microstrip line antenna (b)

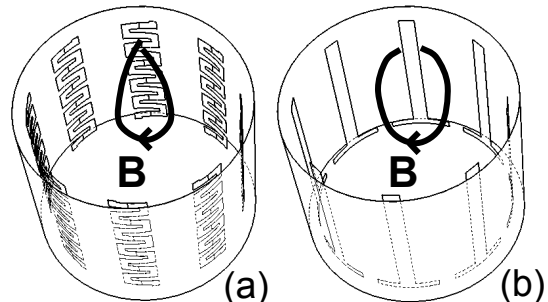


Fig. 4 Magnetic field line of snaking element antenna (a) and microstrip line antenna (b)